Chemical Engineering Journal 159 (2010) 203–211

Contents lists available at ScienceDirect

Chemical Engineering Journal

journal homepage: www.elsevier.com/locate/cej

Pt,In and Pd,In catalysts for the hydrogenation of nitrates and nitrites in water. FTIR characterization and reaction studies

F.A. Marchesini, L.B. Gutierrez, C.A. Querini, E.E. Miró*

Instituto de Investigaciones en Catálisis y Petroquímica, INCAPE (FIQ UNL-CONICET), Santiago del Estero 2829, 3000 Santa Fe, Argentina

ARTICLE INFO

Article history:
Received 28 August 2009
Received in revised form 22 February 2010
Accepted 25 February 2010

Keywords:
Nitrates
Nitrites
Catalytic reduction
CO chemisorption

ABSTRACT

Pt,In and Pd,In catalysts supported on alumina or silica are active for the reduction of nitrate to N_2 in water, using H_2 as reducing agent. The characterization of the catalysts using FTIR of adsorbed CO shows the formation of both linear and bridged CO–Pd and CO–Pt bonds. Besides, carbonate species are formed due to the presence of OH groups provided by the support. The presence of In produces a shift in CO–Pd and CO–Pt bands, suggesting the formation of intermetallic particles. After use in reaction, the amount of CO–Pd and CO–Pt species strongly decreases, the main signals being those associated with carbonate groups. The proportion between bridged and linear species also changes after reaction. These results indicate the agglomeration of metallic particles during reaction, which is in agreement with TEM results.

Increasing the In loading from 0.25 to 0.5 wt.% results in a moderate decrease in the nitrate conversion for all of the catalysts, which could be associated with a decrease of isolated Pd sites which are responsible for the dissociation of hydrogen. The experimental evidence for this point is the decrease of bridged CO adsorbed observed via FTIR for the samples with higher In loading and for all the catalysts.

TPR experiments show low-temperature reduction peaks due to the presence of oxychloride and hydroxychloride particles in monometallic Pd and Pt catalysts. When In is present, the formation of Pd–In and Pt–In compounds provoke the shift of the reduction peaks and the appearance of new reduction signals.

1. Introduction

Nitrates dissolved in water are harmful to human health especially to pregnant women and neonates. Contamination due to both intensive fertilization and waste effluents from industries has produced an increase of nitrate concentration in groundwater. At present, the most widespread technologies for the removal of nitrates are biological denitrification and physical chemical processes: ion exchange, reverse osmosis and electro dialysis. However, they present serious technical problems and can be very expensive. In the last decade, increasing attention has been paid to a novel technology, still in its development stages: catalytic denitrification [1,2] which employs solid bimetallic catalysts. In this catalytic process, nitrates are reduced to nitrogen using hydrogen; however, undesirable products such as nitrite and ammonium are also formed.

Several solid catalysts and process configurations have been reported by various authors [3–5]. The catalysts were prepared over different supports such as massive oxides, alumina, silica and resins, with the addition of Pt or Pd as the main metal, and some second metal such as Cu, Co or In as promoter. The possible mechanism for the catalytic reduction is through the combination of active sites in the bimetallic catalyst [6] where the nitrate is reduced to nitrite over the bimetallic particle, and then the nitrite produced is reduced over the noble metal particle to nitrogen or ammonium depending on site selectivity and environmental conditions. Ammonia is a side product which is obtained due to over-reduction; to avoid this, a strict control of the reaction media is necessary. Nitrate reduction produces hydroxide ions, and the local accumulation of these ions could produce a loss of selectivity and activity.

Recently, it has been reported that the alumina supported Pd,In catalyst is an effective, stable catalyst for nitrate reduction [7]. In a previous work [8], we reported that Pt,In and Pd,In catalysts consist mainly of bimetallic particles with the surface enriched in indium, which was determined mainly using XPS as the characterization tool. These results are in line with those previously reported by Witonska et al. [9] for an alumina supported Pd–In catalyst. They reported that ToF-SIMS measurements showed the presence of intermetallic compounds for catalysts containing 5 wt.% of Pd and different amounts of In promoter.

The aim of this study is to delve into the nature of the active sites and the reaction mechanism of the nitrate reduction over bimetallic Pt,In and Pd,In catalysts. In our previous work, we screened Pd,In and Pt,In catalysts with several compositions and selected

* Corresponding author. Tel.: +54 342 4536861; fax: +54 342 4536861.
E-mail address: emiro@fiq.unl.edu.ar (E.E. Miró).

1385-8947/$ – see front matter © 2010 Elsevier B.V. All rights reserved.
doi:10.1016/j.cej.2010.02.056

the most active ones in order to gain insight into the nature of the active sites and the reaction mechanism. To this end, TPR, TEM and FTIR of adsorbed CO were chosen as characterization tools, activity measurements being carried out in a stirred batch reactor with an on-line pH control. We selected the Pt,In and Pd,In metallic couples because In promoted catalysts have good activity for nitrate conversion and a potential high selectivity to N_2, as reported by other authors [1,6,7].

2. Experimental

2.1. Catalyst preparation

The catalysts were prepared by dry impregnation. Aqueous solutions of H_2PtCl_6 (10 mg mL^{-1}) or $PdCl_2$ (10 mg mL^{-1}), and $InCl_3$ (4.6 mg mL^{-1}) were added to 20–40 mesh particles of SiO_2 or Al_2O_3 at room temperature in order to obtain concentrations of 1 wt.% Pt or Pd and 0.25 or 0.5 wt.% of In. The solids were dried overnight at 120 °C and calcined for 2 h, at 500 °C in air flow. The supports used were 20–40 mesh Al_2O_3 pellets (Ketjen CK300, surface area: 180 m^2 g^{-1}, pore volume: 0.5 mL g^{-1}) or 20–40 mesh SiO_2 pellets (AESAR Large Pore, surface area: 300 m^2 g^{-1}, pore volume: 1 mL g^{-1}).

2.2. Catalyst characterization

Temperature-programmed reduction (TPR) experiments of fresh-calcined samples were performed with 50 mg of catalyst placed in a quartz flow reactor using an Okhura TS 2002 S instrument equipped with a TCD detector. The reducing gas was 5% H_2 in Ar, flowing at 30 mL min^{-1}, and the heating rate was 10 °C min^{-1}. In the case of used samples, the catalysts collected after reaction were dried before performing TPR experiments.

Catalysts TEM images were obtained with a Jeol Electronic Microscopy, Model 100 CX II operating with 6 A resolution. The powder was ultrasonically dispersed in ethanol, and the suspension was deposited on a copper grid.

CO adsorption followed by FTIR analysis was carried out using an IR cell made of glass with CaF_2 windows. The cell consists of a body into which the catalyst wafer can be placed and pretreated with H_2 or evacuated up to 10^{-6} Torr. A temperature controller is connected to the cell oven in order to heat the sample up to the desired temperature. The infrared spectrometer was a Shimatzu IR Prestige 21 instrument and the spectra were collected at a resolution of 8 cm^{-1}. The standard wafer pretreatment was a reduction in a 20 mL min^{-1} of flowing H_2 at 400 °C for 1 h. After that, the reductant gas was stopped and the system was evacuated at 10^{-6} Torr during 30 min keeping the temperature at 400 °C. After collecting a reference spectrum for background subtraction at room temperature, the disk was exposed to an 8 Torr of CO for 15 min. Then, the spectra were collected. This step was repeated at higher CO pressures: 16, 40 and 90 Torr. All the spectra shown in this work were normalized at the same weight/surface wafer ratio.

2.3. Reaction experiments

The reaction test was performed in a three-necked round bottom flask (volume 250 mL) equipped with a magnetic stirrer (700–800 rpm). The pH value was controlled by using an automatic pH controller unit. Experiments were carried out at room temperature, pH 5 and atmospheric pressure. Hydrogen was fed by a tube into the solution.

The catalysts were pretreated under a flow of H_2 (100 mL min^{-1}) at 450 °C with a heating rate of 10 °C min^{-1}. Then, a stirred batch reactor was loaded with 80 mL of distilled water, 200 mg of catalyst, and 100 N-ppm of nitrate as initial concentration. Subsequently, a hydrogen flow of 400 mL min^{-1} was fed to the batch reactor. A pH of ca. 5 was maintained during the reaction time by the addition of small amounts of HCl [7].

Small samples were taken from the vessel for the determination of nitrate, nitrite and ammonium using Vis spectroscopy (Cole Parmer 1100 Spectrophotometer) combined with colorimetric reagents. In order to determine nitrates, the Cd column method and then the colorimetric Gries reaction were used. This colorimetric reaction is the same as the one employed in the assay for nitrites. Ammonium was analyzed by the adapted Berthelot method.

Table 1
TPRs maximum H_2 consumption temperatures.

Catalysts	wt.%	TM (°C)
Pd,In/Al_2O_3	1:0.5	131, 356
	1:0.25	121, 326
Pd,In/SiO_2	1:0.5	114, 369, 507
	1:0.25	118, 322, 418
Pt,In/Al_2O_3	1:0.5	238, 392
	1:0.25	229, 370
Pt,In/SiO_2	1:0.5	127, 348
	1:0.25	127, 315
Pd/Al_2O_3	1	115, 89
Pd/SiO_2	1	111
In/Al_2O_3	0.5	300, 385, 517
In/SiO_2	0.5	378, 469, 565
Pt/Al_2O_3	1	226, 359
Pt/SiO_2	1	120, 176, 352, 494

3. Results and discussion

3.1. Catalysts characterization

3.1.1. TPR results

The redox state of elements and their relative reduction fraction were determined by TPR on both fresh (calcined) and used under reaction catalysts. This technique can be complemented with results obtained with other characterization techniques with which the main species present in Pt,In and Pd,In catalysts have been identified. When the deposition of the metals is performed using chlorinated salts, which is our case, it is known that oxychloride and hydroxychloride compounds remain on the catalyst surface even after calcination [10], giving place to low-temperature reduction peaks that overlap those originated by highly dispersed paladium oxide in the case of paladium catalysts. As a matter of fact, in a XPS characterization of our samples (not shown), we have clearly observed the characteristic Cl 2p signal at 199 eV. The occurrence of Pt,In and Pd,In interactions has also been previously reported using XPS characterization [8]. Thus, we would suggest some correspondence between the TPR signals and the presence of the species mentioned above.

The TPR peaks were characterized by the temperature corresponding to the maximum hydrogen consumption rate (TM). For the used catalysts, the solids were dried at 120 °C before the TPR experiments. Table 1 shows the TM obtained for calcined monometallic and bimetallic catalysts. The description of the TPR profiles of the studied solids is presented in the following sections.

3.1.1.1. Pd,In catalysts. The TPR profiles of the Pd and Pd,In/Al_2O_3 catalysts are shown in Fig. 1A–E. The TPR profile of oxidized Pd/Al_2O_3, Fig. 1A, is characterized by a single reduction peak at TM = 115 °C with a small shoulder at 89 °C. It is known that the reduction of PdO supported over Al_2O_3 takes place at low temperature. In this case, a negative peak associated with βPdH decomposition is detected below 30 °C. These peaks are not

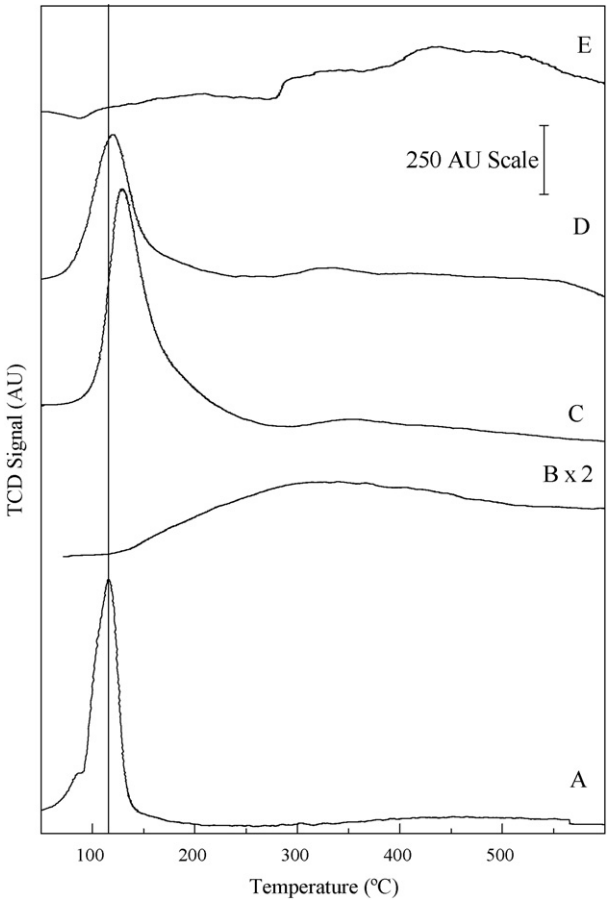

Fig. 1. Temperature-programmed reduction (TPR) of: (A) Pd/Al_2O_3 1 wt.%; (B) In/Al_2O_3 0.9 wt.%; (C) $Pd,In/Al_2O_3$ (1:0.5) wt.%; (D) $Pd,In/Al_2O_3$ (1:0.25) wt.%; (E) $Pd,In/Al_2O_3$ (1:0.25) wt.% used in reaction. Analysis conditions: 30 mL min^{-1} H_2/Ar 5%, heating rate 10 °C min^{-1}.

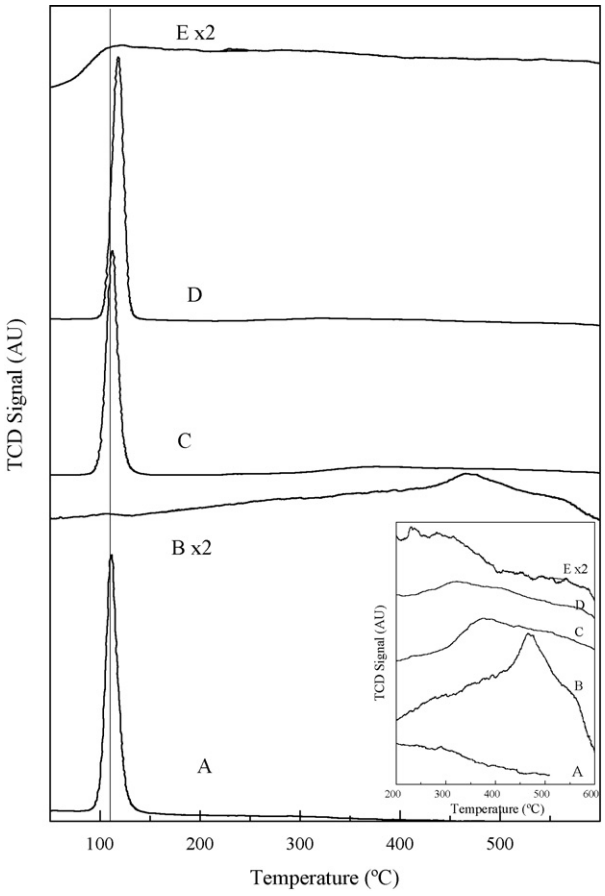

Fig. 2. Temperature-programmed reduction (TPR) of: (A) Pd/SiO_2 1 wt.%; (B) In/SiO_2 0.9 wt.%; (C) $Pd,In/SiO_2$ (1:0.5) wt.%; (D) $Pd,In/SiO_2$ (1:0.25) wt.%; (E) $Pd,In/Al_2O_3$ (1:0.25) wt.% used in reaction. Other conditions: see Fig. 1.

observed in our sample, and the low-temperature peak observed on Pd/Al_2O_3 (Fig. 1A) could be associated with the reduction of palladium oxychloride and hydroxychloride particles over the surface [10]. These compounds came from the precursors used in the catalysts preparation. The TPR profile obtained for oxidized In/Al_2O_3 (Fig. 1B) present two reduction zones: one from 200 to 450 °C with TM at 300 °C assigned to reduction of highly dispersed indium oxidized species and another, not shown, which starts at 600 °C and is associated with the reduction of large particles of In_2O_3 [11]. The profiles obtained on fresh bimetallic catalysts (Fig. 1C and D) present a slight shift to higher temperatures as compared with the Pd sample. As the In loading increases from 0.25 wt.% (Fig. 1D) to 0.5 wt.% (Fig. 1C), the value of TM also increases, from 121 to 131 °C, respectively. The shift of this low-temperature peak can be associated with the formation of Pd–In particles, whose presence has been suggested in [8] through XPS characterization. The same trend is observed for the second peak where TM increases from 326 to 356 °C. The latter peak could be related to particles of indium oxides with different interactions with the Al_2O_3 support.

Fig. 1E shows the TPR profile of the used $Pd,In/Al_2O_3$ (1:0.25) wt.%, where the negative peak of βPdH at low temperature (less than 100 °C) can now be seen. Then, at 204 °C a broad, small signal is observed which could correspond to interacting Pd–In particles which were oxidized after reaction. A broad peak with components at 326, 433 and 512 °C is also observed, associated with different kinds of indium oxide species.

Fig. 2A–E displays TPR profiles of the Pd and Pd,In catalysts supported on SiO_2. As in the Al_2O_3 supported catalysts, a narrow peak is detected at low temperature, which could be associated with chloride-palladium species. For the Pd/SiO_2 sample, this reduction peak has a maximum at 111 °C, and with the addition of indium, this peak also slightly shifts towards higher temperature due to the Pd–In interaction. At higher temperature regions, the peaks corresponding to a reduction of In oxidized species can be observed.

In the $Pd,In/SiO_2$ (1:0.25) wt.% used sample (Fig. 2E), the low-temperature interaction peak seems to disappear and just a small broad peak appears at higher temperature (284 °C), representing the residual indium particles which were oxidized during the reaction.

3.1.1.2. Pt,In catalysts. The TPR profiles of the Pt and $Pt,In/Al_2O_3$ are shown in Fig. 3A–E. Monometallic catalysts, Pt/Al_2O_3 and In/Al_2O_3 (Fig. 3A and B), are compared with fresh bimetallic solids (Fig. 3C and D). Fig. 3A shows two peaks which, in the literature, were assigned to $Pt^{IV}(OH)_xCl_y$ (226 °C) and $Pt^{IV}O_xCl_y$ (359 °C) formed from the chlorined precursors used in the catalyst preparation [12]. In the reduction profiles of bimetallic fresh samples (Fig. 3C and D), it can be observed that the resolution between those two peaks is lost due to the appearance of a third one between them. This band could be associated with the reduction of Pt–In particles.

In the $Pt,In/Al_2O_3$ (1:0.25) wt.% used sample (Fig. 3E), three TMs, 109, 315 and 521 °C can be identified. The first two are related to reduction of some particles of Pt and Pt–In which were oxidized during the reaction, and the latter is related to aggregated In_2O_3 particles. This phenomenon of aggregation results from the interaction with the reaction media as demonstrated in a previous work [13].

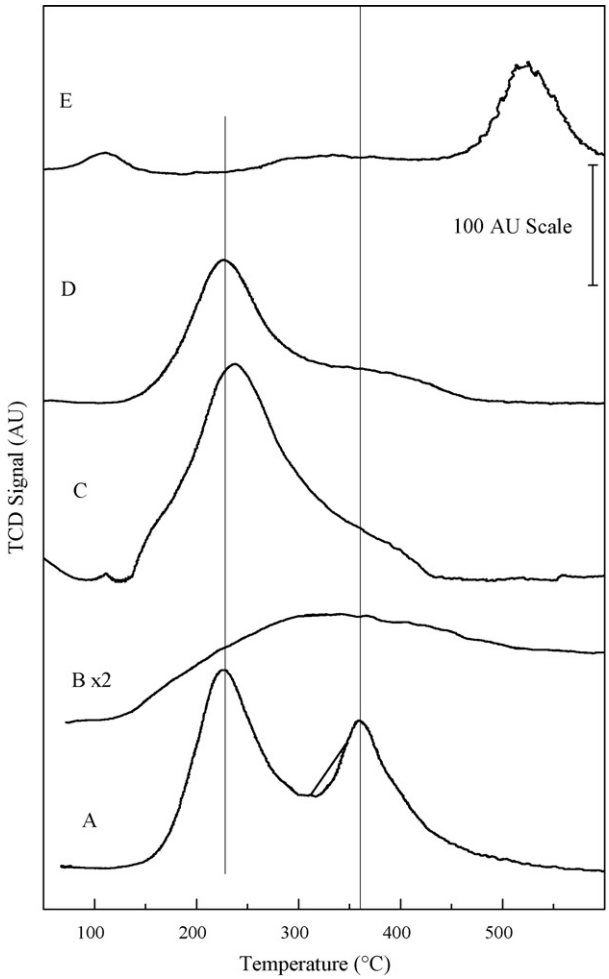

Fig. 3. Temperature-programmed reduction (TPR) of: (A) Pt/Al_2O_3 1 wt.%; (B) In/Al_2O_3 0.9 wt.%; (C) $Pt,In/Al_2O_3$ (1:0.5) wt.%; (D) $Pt,In/Al_2O_3$ (1:0.25) wt.%; (E) $Pt,In/Al_2O_3$ (1:0.25) wt.% used in reaction. Analysis conditions: see Fig. 1.

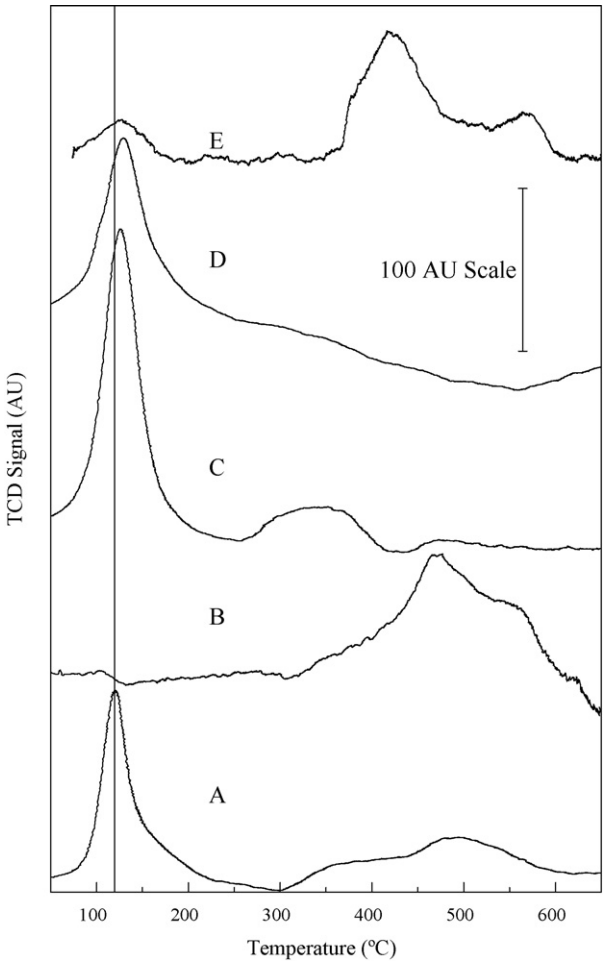

Fig. 4. Temperature-programmed reduction (TPR) of: (A) Pt/SiO_2 1 wt.%; (B) In/SiO_2 0.9 wt.%; (C) $Pt,In/SiO_2$ (1:0.5) wt.%; (D) $Pt,In/SiO_2$ (1:0.25) wt.%; (E) $Pt,In/SiO_2$ (1:0.25) wt.% used sample. Analysis conditions: see Fig. 1.

The TPR profiles of the Pt and $Pt,In/SiO_2$ catalysts are shown in Fig. 4A–E. The fresh Pt/SiO_2 reduction profile presents three peaks (Fig. 4A). The first one at 120 °C is related to small highly dispersed PtO_2 particles. At higher temperatures, there appear two broad signals which could represent the reduction of agglomerated PtO_2 particles which have a strong interaction with the support, or chlorined species as in the alumina supported catalysts.

When In is loaded (Fig. 4C and D), the intermediate-temperature peak shifts to lower temperatures which could be again associated with the formation and reduction of bimetallic Pt–In particles. The peaks appearing at higher temperatures when the Pt/In ratio decreases suggest the presence of not easily reducible bigger particles.

The used $Pt,In/SiO_2$ (1:0.25) wt.% sample (Fig. 4E) shows the same behavior as the other used samples presented before (Figs. 1E, 2E and 3E). It seems that the reduction peak of Pt–In particles almost disappears while the reduction of In_2O_3 increases. These results reveal that Pt particles remain reduced after reaction.

3.1.2. TEM results

The distribution of particle sizes as determined by TEM is presented in Fig. 5. Fig. 5A and B shows the distribution for Pd,In and Pt,In supported on Al_2O_3, while Fig. 5C and D shows the results for Pd,In and Pt,In supported on SiO_2. Besides, results for the same catalysts after being under reaction conditions are shown in the same figures. In all the catalysts, a reorganization of particle sizes appears after reaction, a notorious increase in particle size being observed.

3.1.3. FTIR of adsorbed CO as probe molecule

In order to know the oxidation state of the active compounds and their accessibility on the catalyst surface, CO adsorption was performed followed by FTIR analysis. Some of the main questions to be addressed to understand the behavior of the bimetallic catalysts studied in this work are how indium influences the behavior of Pd and Pt, to what extent Pd–In and Pt–In alloys are formed, and what is the nature of the interactions with the supports.

3.1.3.1. Pd,In catalysts. The CO adsorption spectra on Pd/Al_2O_3 are shown in Fig. 6A. In the 2200–1600 cm^{-1} range, several peaks associated with the CO adsorption on Pd species can be observed. The asymmetric band with maximum at 2092 cm^{-1} assigned to linearly adsorbed CO on atop sites Pd^0 preserves its intensity even if the CO pressure increases, suggesting that the catalyst surface is almost completely covered with CO at the lowest pressure. This band does not change its shape indicating that the palladium particles are highly dispersed.

The signal at the 2020–1800 cm^{-1} range indicates the presence of bridged CO bonding with palladium, forming a Pd^0–CO–Pd^0 complex with different coordinations. The asymmetric band increases with the increment of CO pressure. The bands at 1445 and 1649 cm^{-1}, assigned to surface carbonates, were observed by Sica and Gigola [14] on Pd/Al_2O_3 exposed to CO. In our study,

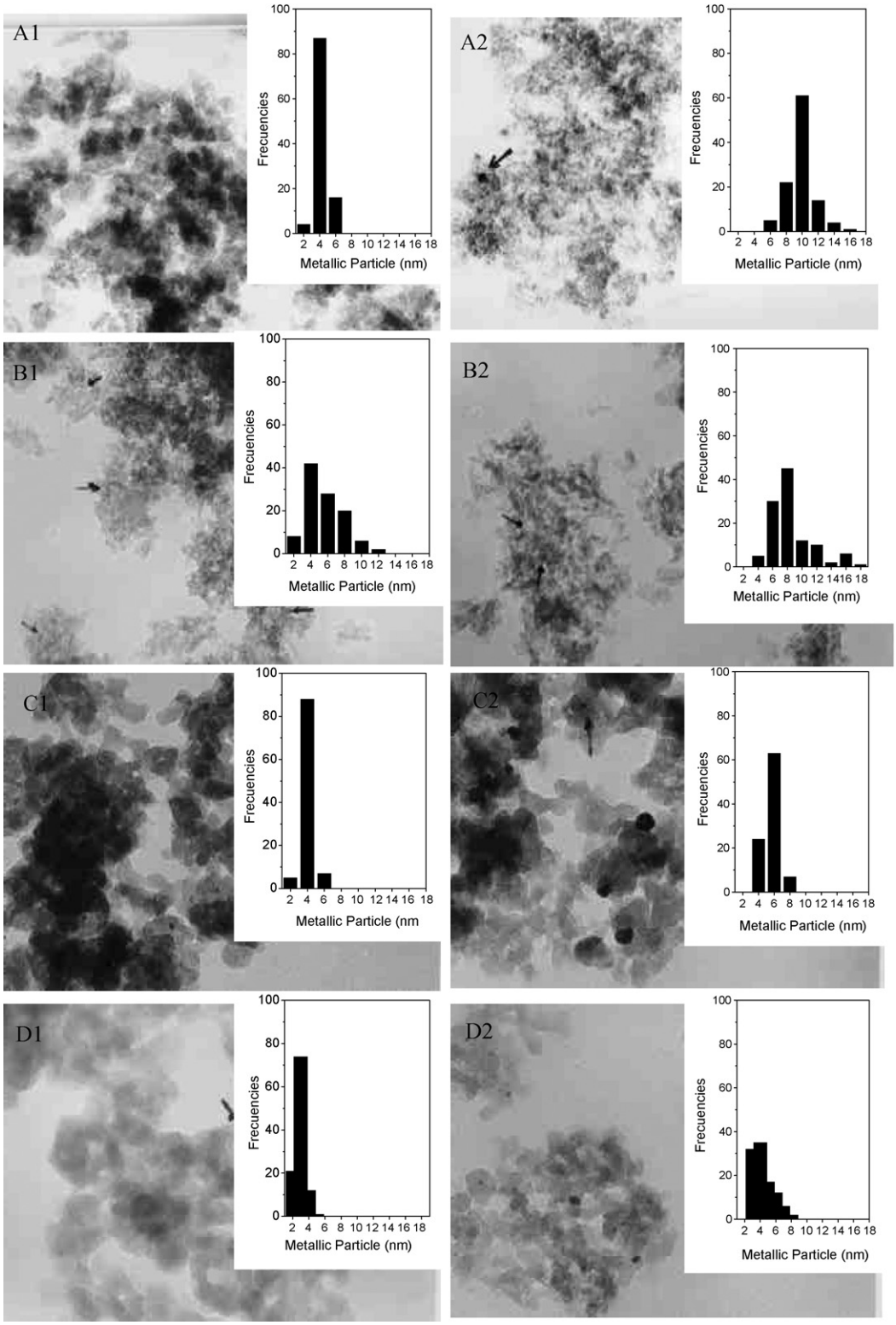

Fig. 5. TEM pictures and the corresponding histograms for fresh and used catalysts. Catalysts supported on Al_2O_3: (A) Pd,In and (B) Pt,In. Catalysts supported on SiO_2: (C) Pd,In and (D) Pt,In. Fresh catalysts: 1; used catalysts: 2. Scale: 1 mm = 4.4 nm.

the adsorption of CO at room temperature on reduced samples develops clear bands at 1647, and at 1437 and 1228 cm^{-1}. Carbonates present as a free CO_3^{2-} ion could be identified by a band at 1437 cm^{-1}. On the other hand, absorption bands located in the 1630–1650 cm^{-1} range are assigned to the stretching frequency ($\nu_{C=O}$) of bridged carbonates. These structures also gave an absorption band at 1220–1270 cm^{-1} due to asymmetric stretching (ν_{asCOO}).

The band at 1647 cm^{-1} can also be associated with the adsorption of CO on the support surface (ν_{CO-OH}), as this band also appears on the reduced Al_2O_3 without any supported metallic cation (Fig. 6).

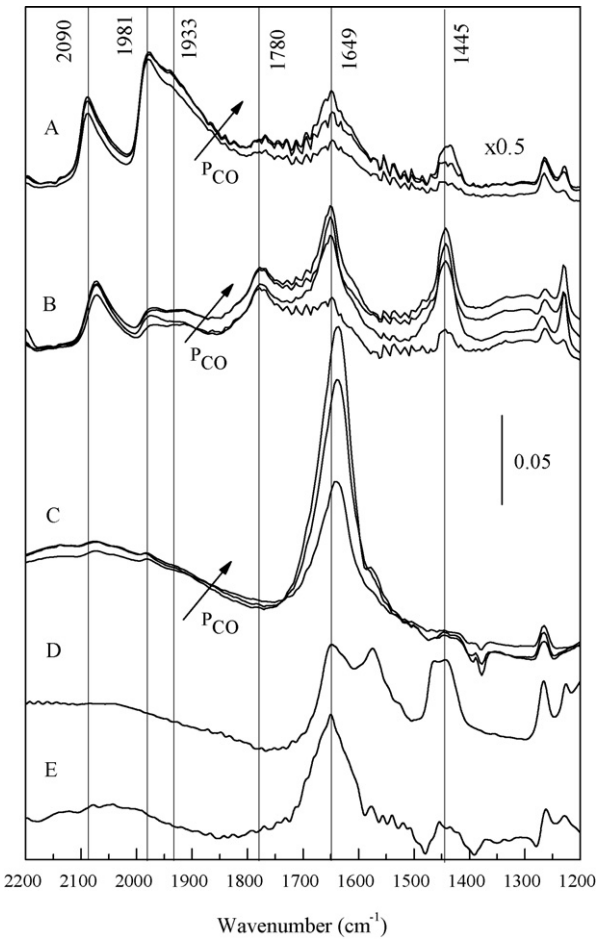

Fig. 6. IR spectra of CO adsorbed on reduced at 400 °C samples: (A) fresh Pd/Al_2O_3: P_{CO} = 16, 40, and 90 Torr; (B) fresh $Pd,In/Al_2O_3$ (1:0.25) wt.%: P_{CO} = 8, 16, 40, and 90 Torr; (C) used $Pd,In/Al_2O_3$ (1:0.25) wt.%: P_{CO} = 16, 40, and 90 Torr; (D) fresh $Pd,In/Al_2O_3$ (1:0.5) wt.%: P_{CO} = 16; (E) Al_2O_3: P_{CO} = 90.

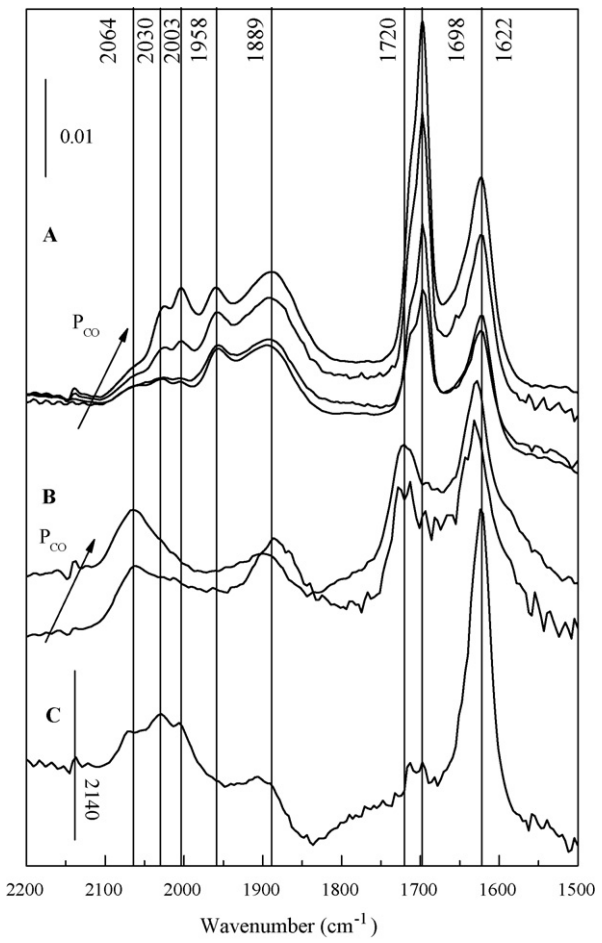

Fig. 7. IR spectra of CO adsorbed on IR spectrum of CO adsorbed on reduced at 400 °C samples: (A) fresh Pd/SiO_2: P_{CO} = 8, 16, 40, and 90 Torr; (B) fresh $Pd,In/SiO_2$ (1:0.25) wt.%: P_{CO} = 40 and 90 Torr; (C) used $Pd,In/SiO_2$ (1:0.25) wt.%: P_{CO} = 90 Torr.

The formation of carbonate and bicarbonate species accounts for the existence of reactive surface oxygen which oxidizes CO to CO_2. The presence of CO_3^{2-} and/or HCO_3^- species on the surface of the impregnated solids indicates that they contain an amount of reducible cation. However, the absence of any detectable signals in the 2100–2150 cm^{-1} range, which is typical of adsorption of CO on oxidized $Pd^{\delta+}$ species, confirms that Pd is fully reduced.

The presence of Indium (0.25 wt.%) in the $Pd,In/Al_2O_3$ catalyst leads to a shift of the CO adsorption band on Pd^0 to lower frequencies, and the relative intensity of the signals which corresponds to bridged bondings decreases drastically. These results indicate that there is an interaction between Pd and In which leads to a decrease in the Pd adsorption capacity. The decrease of the bridged/linear signal ratio might be due to a higher Pd dispersion, or to a geometrical effect of In on the Pd particles. Since the linear CO adsorption also decreases, the latter is the explanation that better explain the results. The bands at the 1200–1800 cm^{-1} range have higher intensities (relative to those in the 2200–1800 cm^{-1} range) than in the monometallic sample, which suggests that some metal alloy was formed together with carbonate species.

On the used catalyst the main band that appears at 1637 cm^{-1}, which also appears on the bare alumina, can be safely assigned to ν_{CO-OH} due to the absence of the other bands that are characteristic of carbonates. This behavior may be attributed to the agglomeration of In surface-enriched Pd–In clusters which leads to an OH concentration increment. The bridged and linear CO signals appear with very weak intensities.

For the Pd/SiO_2 catalyst, Fig. 7A, the CO adsorption spectra do not show the presence of linear CO adsorbed on Pd^0 (2088 cm^{-1}). Either this result could be due to a stronger Pd-SiO_2 interaction (compared to Al_2O_3) or to the fact that in this catalyst palladium dispersion is lower. A band at 1958 cm^{-1} and a shoulder at 1985 cm^{-1} are characteristic of bridging and terminal CO adsorbed on fully reduced Pd, respectively [15].

The bands at 1800–2000 cm^{-1} region might be assigned to CO-bridged-bonded sites associated with different kinds of palladium species while the low intensity bands at 2138 and 2064 cm^{-1} correspond to linearly adsorbed CO. It is well known that on the pure monocrystalline surface, CO is adsorbed in the bridged form mainly, while on Pd small particles a larger intensity of linearly adsorbed CO could be observed. In our solid, the Pd dispersion appears to be very small and, on the other hand, there is a high concentration of free OH on the surface capable of forming carbonate species (1720–1600 cm^{-1}).

The incorporation of Indium, Fig. 7B, produces a slight increment on the dispersion, evidenced by the CO– adsorbed bands at 2065 and 2138 cm^{-1} (linear CO bonding with Pd) and the decrease in intensity of carbonate species which suggests that the surface is more covered by metallic species than by OHs. Additionally, on the used bimetallic catalyst (Fig. 7C), there could be an agglomeration of such bimetallic species as only a high band of free carbonates appears.

3.1.3.2. Pt,In catalysts. Fig. 8B shows the IR spectra of adsorbed CO on the Pt/A_2O_3 catalyst and their changes with the increment of CO

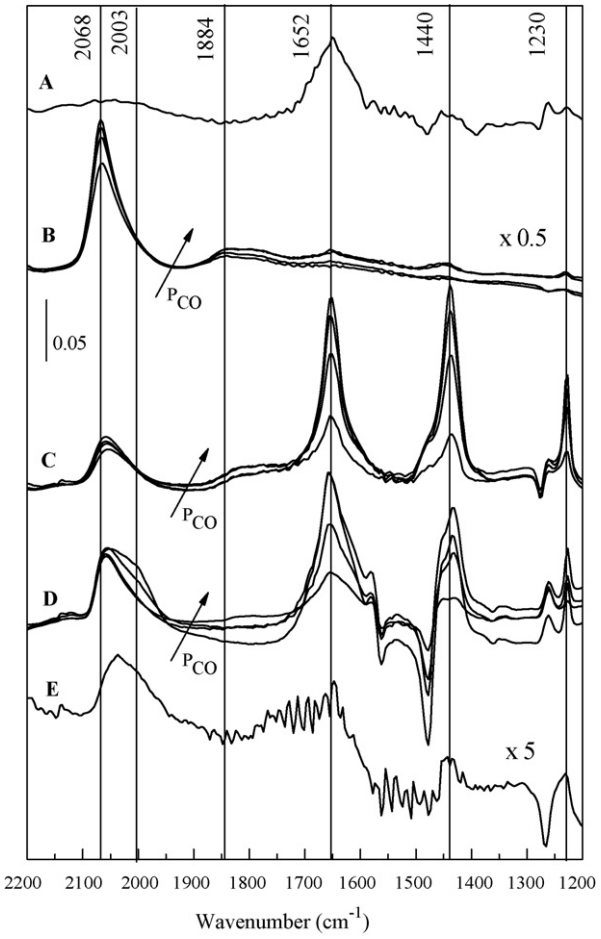

Fig. 8. IR spectrum of CO adsorbed on reduced at 400 °C samples: (A) Al_2O_3: P_{CO} = 90; (B) fresh Pt/Al_2O_3: P_{CO} = 8, 16, 40, and 90 Torr; (C) fresh $Pt,In/Al_2O_3$ (1:0.25) wt.%: P_{CO} = 8, 16, 40, and 90 Torr; (D) used $Pt,In/Al_2O_3$ (1:0.25) wt.%: P_{CO} = 16, 40, and 90 Torr; (E) fresh $Pt,In/Al_2O_3$ (1:0.5) wt.%: P_{CO} = 40.

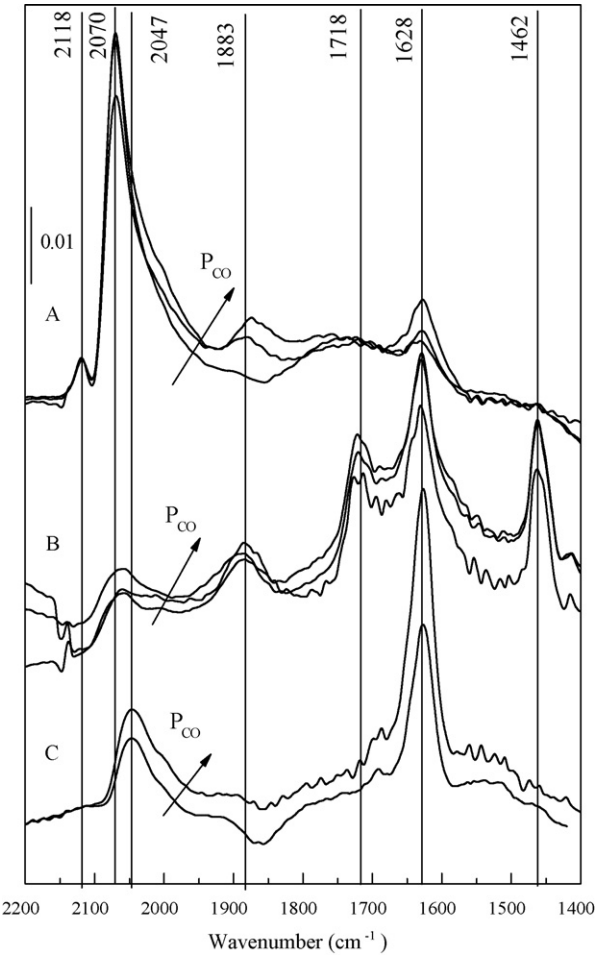

Fig. 9. IR spectrum of CO adsorbed on reduced at 400 °C samples: (A) fresh Pt/SiO_2: P_{CO} = 16, 40, and 90 Torr; (B) fresh $Pt,In/SiO_2$ (1:0.25) wt.%: P_{CO} = 8, 40, and 90 Torr; (C) used $Pt,In/SiO_2$ (1:0.25) wt.%: P_{CO} = 8 and 90 Torr.

pressure. The strong asymmetric band at 2068 cm^{-1} is assigned to CO linearly adsorbed on Pt sites. There is a shoulder on this main peak on the low frequency side at around 2046 cm^{-1}. Haaland [16] attributed the peak doublet to CO adsorbing on two different types of Pt surface sites. The peak at the higher frequency corresponds to CO linearly adsorbed on the flat terraces of the platinum particles, while the broad shoulder was attributed to the CO in Pt atoms situated in high-Miller-index steps or corner of the platinum particles. On the other hand, Balakrishnan and Schwank [17] assigned these bands to CO adsorption on Pt particles that do not possess extended crystal faces because of either their morphology or their very small size. The high frequency signal is probably due to CO adsorption on extended crystalline planes of platinum. The presence of the peak at low frequency was formed by CO adsorption on the Pt that interacts with the support. It should be reasonable to assume that this sample possesses a particle size distribution that is broad, since both peaks were present in the CO adsorption spectra.

There is a broad weak peak located at 1850–1800 cm^{-1} which is attributed to bridged CO species. The intensity of these bands does not change as the CO pressure increases. It should be noticed that no carbon monoxide adsorption at these frequencies occurred on either Al_2O_3 (Fig. 8A) or In/Al_2O_3 (not shown) treated under the conditions applied in this study.

Fig. 8C reports the CO adsorption spectra of the fresh $Pt,In/A_2O_3$ (1:0.25 wt.% catalyst). The deconvolution of the signal between 2200 and 1700 cm^{-1} denotes the presence of two contributions, one at 2063 cm^{-1} and the other at 2029 cm^{-1}. Comparing with the adsorption signals on Pt/Al_2O_3, Fig. 8B, both peaks shifted to lower frequencies and display a lower intensity. The bridged CO species signal present at the 1800–1850 cm^{-1} range is smaller than the one observed on Pt/Al_2O_3. These two features suggest the presence of some interaction of the Pt species with indium.

The spectra of the CO adsorbed on the used $Pt,In/A_2O_3$ (1:0.25) wt.% solid also show a broad peak with two centers at 2059 and 2014 cm^{-1}. The shift to lower frequencies is noticeable, and the peak is broader with the increment of the CO coverage; the signal at the lower frequency (2014 cm^{-1}) is more noticeable suggesting a modification of the surface where palladium in anchored. We can conclude that after use in reaction some redistribution and an increment in particle size have occurred. There was a loss of dispersion as shown by the TEM results which led to an increment of free surface where carbonate species develop. The intensity of the CO adsorption band on both bimetallic samples is almost half-lower than the one observed on the Pt/Al_2O_3 solid, Fig. 8B. This suggests that indium may occlude the Pt particles or that some Pt–In alloy might be formed. The shift may be attributed to an electronic modification of the Pt surface by In.

While the Pt:In ratio decreases from 1:0.25 to 1:0.5 the intensity of the adsorption band on the fresh catalyst decreases, and frequencies shift to lower values (see Fig. 8E). These two observations can be considered as evidence that in the Pt,In samples, Pt and In form a bimetallic particle in which Pt atoms are diluted by In atoms.

The CO adsorption spectra on Pt/SiO_2 are shown in Fig. 9A. The intensity of the signal remains constant while the CO pressure

Table 2
Summary of reaction results, selected from [8].

Catalyst		Residual N-ppm[a]		
		NO_3^-	NO_2^-	NH_4^+
$Pt,In/Al_2O_3$	1:0.5	41.9	1.3	22.0
	1:0.25	40.5	0.6	17.1
$Pt,In/SiO_2$	1:0.5	90.1	1.8	3.3
	1:0.25	73.2	1.9	1.0
$Pd,In/Al_2O_3$	1:0.5	0.4	ND	6.4
	1:0.25	ND	0.1	19.6
$Pd,In/SiO_2$	1:0.5	47.3	0.4	3.3
	1:0.25	9.2	ND	1.3

[a] After 100 min of time-on-stream.

increases, suggesting that the catalyst surface is almost completely covered with CO at the lowest pressure. The asymmetric peaks do not change their shape, thus indicating that the platinum particles are highly dispersed. The main band at 2070 cm^{-1} is followed by a tail, which has two components at 2076 and 2018 cm^{-1}. These bands are directly associated with CO linearly adsorbed on different-size Pt particles [15,16,18].

A small broad signal is observed at lower frequencies (1900–1800 cm^{-1}) assigned to CO bridged bonded on high-dispersed particles.

The bands that appear at 2118 and 2140 cm^{-1} are attributed to CO adsorbed on oxidized Pt surface [18]. Hollins et al. [19] reported that the band at 2120 cm^{-1} is due to CO adsorption on defect sites, steps and corners on the catalyst surface. This signal may be due to the presence of Pt^{2+} with strong interaction with the support. This is in agreement with TPR results, which showed a broad reduction peak zone at temperatures higher than 400 °C.

When In is added (0.25 wt.%), Fig. 9B, the spectra of the fresh solid show a low intensity broad band with a maximum at 2070 cm^{-1} and the contribution of two peaks at 2052 and 2018 cm^{-1}. While on the used catalyst the adsorption band at 2070 cm^{-1} completely disappears, the broad peak is formed by a signal at 2046 cm^{-1} (Fig. 9C).

On the fresh solid, Fig. 9B, the band at 2140 cm^{-1} is very small, but it is absent in the used catalyst (see Fig. 9C), and there is no band at 2118 cm^{-1}.

The frequency of the CO adsorption bands and their intensity decrease when indium is incorporated to the Pt/SiO_2 solid and these features are smaller on the used bimetallic catalyst $Pt,In/SiO_2$ (1:0.25) wt.%. This result suggests that during the reaction some reorganization in the position and size distribution occurs, probably with loss of particle dispersion and with the indium being concentrated on top of platinum particles, blocking the adsorption centers.

Shifts in the CO band position are generally interpreted as evidence of changes in the electronic properties of supported metals. The exact position of the adsorption bands depends on parameters such as particle size, surface coverage and electronic changes in the metal structure. In our catalysts, the presence of indium leads to a strong Pt–In interaction leading to a sort of Pt–In alloy and carbonate species formation.

3.2. Reaction studies

In a previous work, we screened Pd,In and Pt,In catalysts with several compositions, and we selected the most active ones in order to gain insight into the nature of the active sites and the reaction mechanism. Table 2 shows a summary of catalytic results for the catalysts studied in this work. In general, we have reported that Pd,In catalysts reduce nitrates faster than Pt,In ones, and alumina

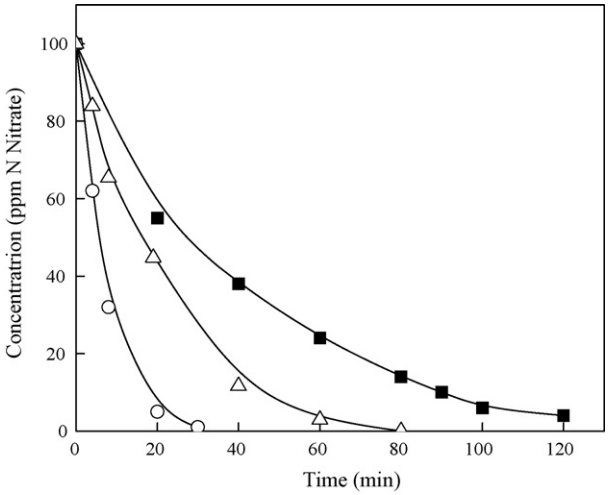

Fig. 10. Nitrate hydrogenation over Pd,In (1:0.25) using different catalyst loadings. (■) 0.1 g; (△) 0.2 g; (○) 0.4 g. For other reaction conditions see Section 2.

seems to be a better support than silica, which could be due to the higher PZC value of silica, thus decreasing the rate of adsorption of nitrate ions. Catalysts containing only noble metals (Pt or Pd) are almost inactive. The addition of a small amount of In to Pt/Al_2O_3 and Pd/Al_2O_3 increases nitrate conversion. However, the addition of higher amounts of In results in lower conversions [8]. Among the catalysts studied in our previous work [8], $Pd,In/Al_2O_3$ (1:0.25) wt.% presented the best catalytic activity for nitrate conversion, the monometallic Pd/Al_2O_3 catalyst being almost inactive. Fig. 10 shows the nitrate conversions obtained for this catalyst. It can be observed that, when the amount of catalyst is increased, total nitrate conversion can be reached in shorter times, which suggests that mass transport does not pose severe limitations in the nitrate hydrogenation.

In general, it is accepted that the reaction mechanism involves the reduction of nitrate into nitrite, which is in turn reduced towards nitrogen or over-reduced to give ammonia, which is a non-desired product [20]. Thus, the selectivity of the reaction is related to the ability of the catalyst to selectively hydrogenate nitrite into nitrogen. In this vein, Fig. 11 shows results obtained for nitrite reduction over the $Pd,In/Al_2O_3$ (1:0.25) wt.% catalyst. While for nitrate hydrogenation total conversion is reached after ca. 40 min, nitrites are totally consumed after only 20 min of reaction. Surprisingly, the production of ammonia increases somewhat after the nitrite is totally depleted, which suggests that either nitrites remain adsorbed at the catalyst surface yielding ammonia or that ammonia remains adsorbed and is released towards the solution after the reaction is completed. Recently, Miyazaki et al. [21] reported that nitrites are readily adsorbed on the surface of alumina-based catalysts, thus this adsorption could be the explanation for the observation made above.

Prüsse and Vorlop [22] suggested that for the Pd,Cu catalyst, bimetallic centers are necessary for the reduction of nitrate to nitrite, the Pd isolated centers being necessary for the activation of the hydrogen and for the reduction of the formed nitrites. These concepts could also be applied to our Pd,In and Pt,In catalysts.

Increasing the In loading from 0.25 to 0.5 wt.% results in a moderate decrease in the nitrate conversion for all of the catalysts (Table 2), which could be associated with a decrease of isolated Pd sites which are responsible for the dissociation of hydrogen. The experimental evidence for this point is the decrease of linear CO adsorbed, observed via FTIR for the samples with higher In loading and for all the catalysts. On the other hand, a high amount of isolated Pd or Pt may have a negative effect, which is an increase in

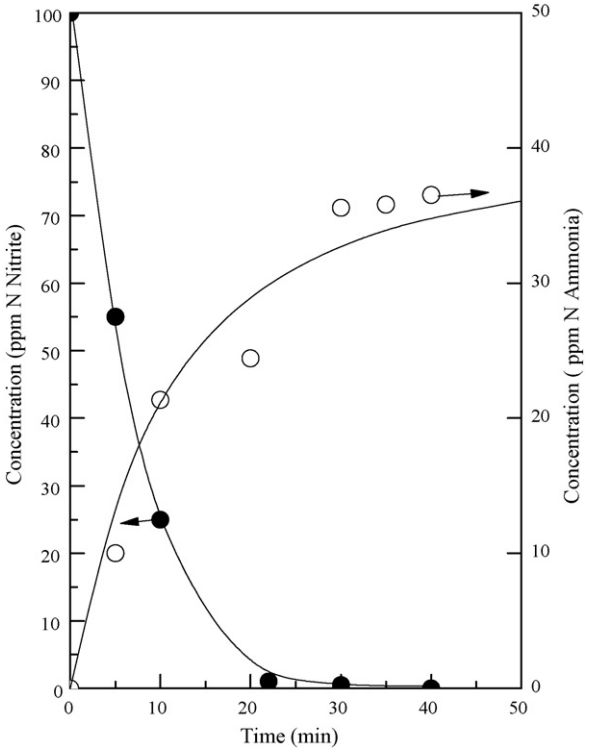

Fig. 11. Nitrite reduction and ammonia production on In(0.25 wt.%) promoted Pd(1 wt.%) catalyst supported on Al_2O_3; (●) ppm N Nitrite; (○) ppm N Ammonia. For reaction conditions see Section 2.

ammonium production due to the availability of dissociated hydrogen. Thus, the rate of each step in the reaction network is strongly dependent on the availability of hydrogen at the catalyst surface. Therefore, the metal particle composition can be a key point in the development of active and selective catalysts for this reaction [8]. Actually, it has been established that In decreases the adsorption of hydrogen on platinum and on palladium [19] and, as seen in Table 2 (excluding Pd,In/Al_2O_3 (1:0.25) wt.%), the higher the In content, the lower the NH_4^+. Moreover, FTIR spectra for the catalysts supported on silica show lower amounts of linear CO adsorbed than those supported on alumina, and the production of ammonia is lower when silica is the support.

4. Conclusions

FTIR of adsorbed CO shows the formation of both linear and bridged CO–Pd and CO–Pt bonds at the catalyst surface. Carbonate species are also formed due to the presence of OH groups provided by the support. The presence of In produces a shift in CO–Pd and CO–Pt bands, suggesting the formation of intermetallic particles. Increasing the In loading produces a decrease of linear CO adsorbed for all the catalysts. Thus, the decrease of catalytic activity when the In loading increases could be associated with a decrease of isolated Pd sites which are responsible for the dissociation of hydrogen.

For used catalysts, the amount of CO–Pd and CO–Pt species strongly decreases, the main signals being those associated with carbonate groups. The proportion between bridged and linear species also changes after reaction. These results indicate the agglomeration of metallic particles during reaction, which is in agreement with TEM results.

A shift between nitrite consumption and ammonia production is observed, which is most probably originated in the nitrite adsorption on alumina support.

The composition of bimetallic particles, which regulates the nitrate and nitrite conversion processes, can be a key point in the development of active and selective catalysts for this reaction. Future work is underway using a packed-bed reactor in order to obtain a more complete description of the reaction mechanism and the corresponding kinetic model.

Acknowledgements

The authors wish to acknowledge the financial support received from ANPCyT, UNL and CONICET. They are also grateful to the Japan International Cooperation Agency (JICA) for the donation of the major instruments used in this study. Thanks are given to Elsa Grimaldi for the English language editing and to Claudio Maitre for technical assistance.

References

[1] A. Pintar, J. Batista, Catal. Today 53 (1999) 35.
[2] O. Ilinitch, P. Cuperus, L. Nosova, E. Gribov, Catal. Today 56 (2000) 137.
[3] F. Deganello, L. Liotta, A. Macaluso, A. Venezia, G. Deganello, Appl. Catal. B: Environ. 24 (2000) 265.
[4] Y. Matatov-Meytal, V. Barelko, I. Yuranov, M. Sheintuch, Appl. Catal. B: Environ. 27 (2000) 127.
[5] G. Strukul, R. Gavagnin, F. Pinna, E. Modaferri, S. Perathoner, G. Centi, M. Marella, M. Tomaselli, Catal. Today 55 (2000) 139.
[6] U. Prüsse, M. Hahnlein, J. Daum, K. Vorlop, Catal. Today 55 (2000) 79.
[7] B.P. Chaplin, J.R. Shapley, Catal. Lett. 130 (2009) 56.
[8] F.A. Marchesini, S. Irusta, C. Querini, E. Miró, Appl. Catal. A: Gen. 348 (1) (2008) 60.
[9] I. Witonska, S. Karski, J. Rogowski, N. Krawczyk, J. Mol. Catal. A: Chem. 287 (1–2) (2008) 87.
[10] F.B. Noronha, M. Baldanza, R. Monteiro, D. Aranda, A. Ordine, M. Schmal, Appl. Catal. A: Gen. 210 (2001) 275.
[11] P. Park, C. Ragle, C. Boyer, M. LouBalmer, M. Engelhard, D. McCready, J. Catal. 210 (2002) 97.
[12] H. Lieske, G. Lietz, H. Spindler, J. Volter, J. Catal. 81 (1983) 8.
[13] F.A. Marchesini, C.A. Querini, E.E. Miró, F.G. Requejo, J.M. Ramallo-López, Catal. Commun. 10 (3) (2008) 355.
[14] A.M. Sica, C.E. Gigola, Appl. Catal. A: Gen. 239 (1–2) (2003) 121.
[15] O.S. Aleexeev, S. Krishnamoorthy, C. Jensen, M.S. Ziebarth, G. Yaluris, T.G. Roberie, M.D. Amiridis, Catal. Today 127 (1–4) (2007) 176.
[16] D.M. Haaland, Surf. Sci. 185 (1987) 1.
[17] K. Balakrishnan, J. Schwank, J. Catal. 138 (1992) 491.
[18] J. Lauterbach, G. Bonilla, T.D. Pletcher, Chem. Eng. Sci. 54 (1999) 4501.
[19] P. Hollins, K. Davies, J. Pritchard, Surf. Sci. 138 (1984) 75.
[20] J. Wärnå, I. Turunen, T. Salmi, T. Maunula, Chem. Eng. Sci. 49 (24B) (1994) 5763.
[21] A. Miyazaki, T. Asakawa, I. Balint, Appl. Catal. A: Gen. 363 (2009) 81.
[22] U. Prüsse, K.-D. Vorlop, J. Mol. A: Chem. 173 (2001) 313.